(12)

NUSC Technical Report 7981
21 September 1987

Systolic Array Adaptive Beamforming

Norman L. Owsley
Surface Ship Sonar Department

Naval Underwater Systems Center
Newport , Rhode Island / New London, Connecticut

PREFACE

This report was prepared under NUSC Job Order No. A60050 and was sponsored by ONT (Theo Kooij, Program Manager) and DARPA (Charles Stuart, Program Manager). The NUSC Principal Investigator was Norman Owsley (Code 2111).

The systolic array computer architecture for implementation of the MVDR algorithm originated at ESL, Inc., Sunnyvale, CA. The collaboration with Phil Kuekes (ESL), Doug Kandle (ESL), H. T. Kung (Carnegie Mellon University), and Robert Schreiber (Stanford University) is gratefully acknowledged.

The Technical Reviewer for this report was T. Choinski (Code 2135).

REVIEWED AND APPROVED: 21 September 1987

F. J. Kingsbury

F. J. KINGSBURY
HEAD: SUBMARINE SONAR DEPARTMENT

The author of this report is located at the
New London Laboratory, Naval Underwater Systems Center,
New London, CT 06320.

UNCLASSIFIED

SECURITY CLASSIFICATION OF THIS PAGE

REPORT DOCUMENTATION PAGE

1a. REPORT SECURITY CLASSIFICATION UNCLASSIFIED	1b. RESTRICTIVE MARKINGS
2a. SECURITY CLASSIFICATION AUTHORITY	3. DISTRIBUTION / AVAILABILITY OF REPORT Approved for public release; distribution is unlimited.
2b. DECLASSIFICATION / DOWNGRADING SCHEDULE	
4. PERFORMING ORGANIZATION REPORT NUMBER(S) NUSC TR 7981	5. MONITORING ORGANIZATION REPORT NUMBER(S)
6a. NAME OF PERFORMING ORGANIZATION Naval Underwater Systems Center 6b. OFFICE SYMBOL (If applicable) 2111	7a. NAME OF MONITORING ORGANIZATION
6c. ADDRESS (City, State, and ZIP Code) New London Laboratory New London, CT 06320	7b. ADDRESS (City, State, and ZIP Code)
8a. NAME OF FUNDING / SPONSORING ORGANIZATION ONT and DARPA 8b. OFFICE SYMBOL (If applicable)	9. PROCUREMENT INSTRUMENT IDENTIFICATION NUMBER
8c. ADDRESS (City, State, and ZIP Code) Arlington, VA	10. SOURCE OF FUNDING NUMBERS PROGRAM ELEMENT NO. 62314N PROJECT NO. A60050 TASK NO. RJ14A18 /NU3B WORK UNIT ACCESSION NO. TD0925

11. TITLE (Include Security Classification)

SYSTOLIC ARRAY ADAPTIVE BEAMFORMING

12. PERSONAL AUTHOR(S)
Owsley, Norman L.

13a. TYPE OF REPORT	13b. TIME COVERED	14. DATE OF REPORT (Year, Month, Day)	15. PAGE COUNT
RDT&E	FROM ____ TO ____	1987 September 29	30

16. SUPPLEMENTARY NOTATION

17. COSATI CODES		
FIELD	GROUP	SUB-GROUP

18. SUBJECT TERMS (Continue on reverse if necessary and identify by block number)

Adaptive, Beamforming, Array, Cholesky, Backsolve, Systolic

19. ABSTRACT (Continue on reverse if necessary and identify by block number)

A computing architecture which reflects the specific requirements of an optimum adaptive space-time array processor is discussed. Specifically, a frequency domain implementation of the minimum variance distortionless response (MVDR) beamformer is described. Two systolic computing arrays are presented which implement respectively a rank one update of the Cholesky factor for a spatial sensor array cross-spectral covariance matrix and the solution of a set of linear equations for the optimum array matrix filter beamformer operation. The theoretical performance of the MVDR beamformer is reviewed. Finally, an array partitioning approach permits the application of systolic MVDR beamforming to arrays with very large numbers of sensors is proposed. Two sub-optimum MVDR processes are considered which exhibit nearly optimum performance at high interference-to-noise ratios.

20. DISTRIBUTION / AVAILABILITY OF ABSTRACT	21. ABSTRACT SECURITY CLASSIFICATION
☐ UNCLASSIFIED/UNLIMITED ☒ SAME AS RPT. ☐ DTIC USERS	UNCLASSIFIED

22a. NAME OF RESPONSIBLE INDIVIDUAL	22b. TELEPHONE (Include Area Code)	22c. OFFICE SYMBOL
Norman L. Owsley	(203) 440-4677	2111

DD FORM 1473, 84 MAR — 83 APR edition may be used until exhausted. All other editions are obsolete.

SECURITY CLASSIFICATION OF THIS PAGE
UNCLASSIFIED

TABLE OF CONTENTS

	Page
LIST OF ILLUSTRATIONS	ii
INTRODUCTION	1
THEORY AND DIRECT IMPLEMENTATION	2
SYSTOLIC IMPLEMENTATION	6
PERFORMANCE OF AN MVDR BEAMFORMER	16
ADAPTIVE BEAMFORMING FOR VERY LARGE ARRAYS	17
CONCLUSIONS	26
REFERENCES	28

LIST OF ILLUSTRATIONS

Figure		Page
1	Boundary Cell and Internal Cell Input-Process-Output Diagram for the Cholesky Factor Update	11
2	Linear Systolic Array for a Rank One Cholesky Factor Update. .	12
3	Linear Equation Backsubstitution	14
4	Systolic Array for Solution of Linear Equations by Backsubstitution for a 4-Element Partition	15
5	Minimum Variance Optimum Beamformer AGI Relative to a CBF as a Function of the Interference-to-Noise Ratio for a PIN Measured at the Output of a CBF Steered Directly at the Interference.	18
6	Subarray Space Partitioning and Cascaded Beamforming of a Very Large N-Element Array to Reduce N/P-Input MVDR Beamformer Complexity and Convergence Time Restrictions. Each of (N/P) Subarrays Consists of P Elements With Conventional Beamforming	22
7	Comparisons of Suboptimum (Subarray and Beam Space) and Optimum (Element Space) MVDR Process AGI Versus Interference-to-Noise Ratio	26

SYSTOLIC ARRAY ADAPTIVE BEAMFORMING

INTRODUCTION

Optimum algorithms for the space-time processing requirements of a discrete sensor array have existed in one form or another for almost twenty-five years [Ref. 1]. The computational requirements for implementation have inhibited the widespread application of these techniques to broadband arrays. To date, the hardware realization of the intensive linear algebra operations required for any type of modern signal processing function has not been amenable to cost effective solutions. In this regard, the most promising new development in modern signal processor design has been the result of rapid progress in very large scale integration (VLSI) technology. Large scale integration has allowed the fabrication of special purpose components which has provided the impetus for the evolution of very powerful special purpose computing architectures for linear algebra intensive signal processing requirements [Ref. 2]. While this field represents an area of current intensive research, some concepts, such as the systolic computing cellular array, have already produced significant developments [Ref. 3].

The systolic array and related wavefront processor are specifically designed to exploit the unique regularities of a particular linear algebra operation [Ref. 4]. In particular, a characteristic of many matrix algebra operations is the requirement for data communication between only nearest neighbor arithmetic cells in a properly designed array of such cells. This basic principle of simplification in conjunction with the relatively low cost of VLSI arithmetic cell components makes it feasible to design hardwired systolic array algorithms with essentially no internal control, minimal memory, and maximal parallelism. As a case in point, this report discusses the broadband minimum variance distortionless response (MVDR) beamforming algorithm that consists of the following three matrix

operations: Cholesky factorization of an estimated cross-spectral density matrix (CSDM), solution of a least-squares (filter) problem after each rank one update of the CSDM, and an N-channel matrix filter operation.

First, the theory and direct element level implementation of the adaptive broadband MVDR beamformer is presented, then the systolic array implementation is described. This is followed by a discussion of the theoretical performance predictions for an MVDR process. Finally, some implications of systolic array architectures with respect to variations of the MVDR algorithm for high resolution space-time processing in very large arrays are considered.

THEORY AND DIRECT IMPLEMENTATION

A convenient discrete frequency domain representation of the broadband data from an N-sensor array is given by the vector $\underline{x}_k$ with transpose $\underline{x}_k^T$ specified by

$$\underline{x}_k^T = [x_{1k}(\omega_1) \cdots x_{Nk}(\omega_1) x_{1k}(\omega_2) \cdots x_{Nk}(\omega_2) \cdots x_{1k}(\omega_M) \cdots x_{Nk}(\omega_M)]$$

$$= [\underline{x}_{1k}^T \ \underline{x}_{2k}^T \cdots \underline{x}_{Mk}^T] \ , \tag{1}$$

where

$$x_{ik}(\omega_m) = \frac{1}{\sqrt{T}} \int_{t_k - \frac{T}{2}}^{t_k + \frac{T}{2}} x_i(t) e^{-j\omega_m t} \, dt \ , \tag{2}$$

with $x_i(t)$ the output time-domain waveform of the i-th sensor and ω_m the

m-th discrete radial frequency

$$\omega_m = 2\pi m/T \quad 0 \leq m \leq M-1. \tag{3}$$

Therefore, the elements of the vector $\underline{x}_k$ are seen to be the discrete Fourier coefficients of $x_i(t)$ over the interval $(t_k - T/2, t_k + T/2)$. When the observation time, T, is large with respect to the inverse bandwidth of $x_i(t)$, the Fourier coefficients between frequencies become uncorrelated. We shall assume that this condition is satisfied and that the waveforms $x_i(t)$, $1 \leq i \leq N$, while not necessarily Gaussian random processes, are zero-mean and wide sense stationary.

Consistent with the above waveform assumptions, the covariance matrix $R_m = R(\omega_m)$ at frequency ω_m, hereafter referred to as CSDM, is defined with ij-th element $E[x_{ik}(\omega_m)x^*_{jk}(\omega_m)]$. The covariance matrix for the Fourier coefficient vector $\underline{x}_k$ is an MN-by-MN block diagonal matrix with the CSDM R_m as the m-th N-by-N main block diagonal element. The MVDR beamformer filter $\underline{w}_k$ at time t_k is now defined in terms of the complex conjugate transpose (indicated by superscript H) as

$$\begin{aligned}\underline{w}_k^H &= [w^*_{1k}(\omega_1) \cdots w^*_{Nk}(\omega_1) w^*_{1k}(\omega_2) \cdots w^*_{Nk}(\omega_2) \cdots w^*_{1k}(\omega_M) \cdots w^*_{Nk}(\omega_M)] \\ &= [\underline{w}_{k1}^H \ \underline{w}_{k2}^H \cdots \underline{w}_{kM}^H] \ .\end{aligned} \tag{4}$$

The total broadband output power of the MVDR beamformer is defined as the variance

$$\begin{aligned}\sigma^2 &= E[|\underline{w}_k^H \underline{x}_k|^2] \\ &= \underline{w}_k^H E[\underline{x}_k \underline{x}_k^H] \underline{w}_k\end{aligned}$$

$$= \sum_{m=1}^{M} \underline{w}_{mk}^{H} R_m \underline{w}_{mk} . \qquad (5)$$

The requirement for a distortionless spectral response to a signal with the steering vector $\underline{d}_{mp}$ at frequency ω_m is equivalent to the constraint

$$\mathrm{Re}[\underline{w}_{mk}^{H} \underline{d}_{mp}] = 1 \quad \text{and} \quad \mathrm{Im}[\underline{w}_{mk}^{H} \underline{d}_{mp}] = 0, \; 1 \leq m \leq M \qquad (6)$$

on the MVDR filter weight vector $\underline{w}_{mk}$. The steering vector $\underline{d}_{mp}$ has the n-th element $\exp(j\omega_m \tau_{np})$ where τ_{np} is the relative time delay to the n-th sensor for a signal from the p-th direction. Using the method of undetermined Lagrange multipliers, σ^2 of Eq. (5) is minimized subject to the constraints of Eq. (6) if the criterion function

$$v = \sum_{m=1}^{M} [\underline{w}_{mk}^{H} R_m \underline{w}_{mk} + 2\lambda_{Rm} (\mathrm{Re}[\underline{w}_{mk}^{H} \underline{d}_{mp}] - 1) + 2\lambda_{Im} (\mathrm{Im}[\underline{w}_{mk}^{H} \underline{d}_{mp}])] \qquad (7)$$

is minimized with respect to the real and imaginary parts of $\underline{w}_{mk}$, simultaneously. The solution to this problem is known to be

$$\underline{w}_{mpk} = R_m^{-1} \underline{d}_{mp} / \underline{d}_{mp}^{H} R_m^{-1} \underline{d}_{mp} , \; 1 \leq m \leq M , \qquad (8)$$

where the beam index p indicates that a unique beam/filter vector $\underline{w}_{mpk}$ is required for each of the B ($1 \leq p \leq B$) beam steering signal directions. The corresponding minimum total beamformer broadband output power (variance)

obtained using Eq. (8) in Eq. (5) is

$$b_p^2 = \sum_{m=1}^{M} (\underline{d}_{mp}^H R_m^{-1} \underline{d}_{mp})^{-1}. \tag{9}$$

Therefore, the estimated signal autopower spectral density at frequency ω_m is

$$b_{mp}^2 = (\underline{d}_{mp}^H R_m^{-1} \underline{d}_{mp})^{-1}. \tag{10}$$

In practice, the CSDM matrix cannot be estimated exactly by time averaging because the random process $x_n(t)$ is never truly stationary and/or ergodic. As a result, the available averaging time is limited. Accordingly, one approach to the time-varying adaptive estimation of R_m at time t_k is to compute the exponentially time averaged estimator of the CSDM R_m at time t_k as

$$R_{mk} = \mu R_{m,k-1} + (1 - \mu) \underline{x}_m \underline{x}_m^H , \tag{11}$$

where μ is a smoothing factor ($0 < \mu < 1$) that implements the exponentially weighted time averaging operation. Eq. (11) is a rank one update time averaging operation to the CSDM at frequency ω_m and requires approximately $MN^2/2$ complex multiply-addition operations and an equivalent memory size. The estimator R_{mk} is used in Eqs. (8), (9), and (10) to compute the MVDR filter weights, broadband beamformer output power, and estimated signal spectrum, respectively. A straightforward inversion of R_{mk} requires on the order of MN^3 operations. Approximately BMN^2 additional operations are required to form the beam filter vectors in Eq. (8) and beampower estimates in Eq. (9) for a system with B beams. The average number of operations for the direct implementation of the broadband MVDR beamformer

is, therefore, on the order of

$$O_d = M((N^2/2) + BN^2 + (BN^2 + N^3)/K)$$

$$\approx MN^2 (B + (B + N)/K) \qquad (12)$$

per beamformer update cycle. The parameter K is the number of update cycles of the estimated CSDM R_m between computations of the updated filter weights and beam output power estimates.

SYSTOLIC IMPLEMENTATION

In terms of systolic computing array functions, implementation of the MVDR beamformer does not substantially reduce the computational burden indicated by Eq. (12). Instead, systolic computing exposes the regularity of a particular function in such a way as to make that function amenable to the maximum of parallel computation and a minimum of both control and data transfer. In the following, the primary systolic computing elements are developed.

First, consider the requirement to compute the estimated output power for the m-th frequency, p-th beam steering direction, and k-th update cycle from the beam output power estimate

$$b_{mpk} = 1/g_{mpk}$$

where

$$g_{mpk} = \underline{d}_{mp}^H R_{mk}^{-1} \underline{d}_{mp}. \qquad (13)$$

In the systolic implementation to be described the inverse CSDM R_{mk}^{-1} is never formed explicitly. Rather the upper triangular Cholesky factor U_{mk} of R_{mk}, defined by

$$R_{mk} = U_{mk}^H U_{mk}, \tag{14}$$

is obtained directly (as explained later). The diagonal elements of the Cholesky factor are real. Substituting Eq. (14) into (13) yields

$$\begin{aligned} g_{mpk} &= ((U_{mk}^H)^{-1} \underline{d}_{mp})^H ((U_{mk}^H)^{-1} \underline{d}_{mp}) \\ &= \underline{v}_{mpk}^H \underline{v}_{mpk} \\ &= |\underline{v}_{mpk}|^2 , \end{aligned} \tag{15}$$

where only the complex vector $\underline{v}_{mpk} = (U_{mk}^H)^{-1} \underline{d}_{mp}$ must be computed at a cost of $MN^2/2$ operations. To form the beam output from the beam filter vector of Eq. (8), i.e.,

$$\begin{aligned} y_{mpk} &= \underline{w}_{mpk}^H \underline{x}_{mk} \\ &= \underline{d}_{mp}^H R_{mk}^{-1} \underline{x}_{mk}/g_{mpk}, \end{aligned}$$

again use the Cholesky factorization of Eq. (14) to obtain

$$\begin{aligned} y_{mpk} &= ((U_{mk}^H)^{-1} \underline{d}_{mp})^H ((U_{mk}^H)^{-1} \underline{x}_{mk})/g_{mpk} \\ &= \underline{v}_{mpk}^H \underline{z}_{mpk}/|\underline{v}_{mpk}|^2. \end{aligned} \tag{16}$$

The important point with respect to Eq. (16) is that the computation of the vector

$$\underline{z}_{mpk} = (U_{mk}^H)^{-1} \underline{x}_{mk} \tag{17}$$

is of the exact form as that for

$$\underline{v}_{mpk} = (U_{mk}^H)^{-1} \underline{d}_{mp} \tag{18}$$

in Eq. (15). Thus, the same circuitry can be used for each computation.

A realization of the MVDR beamformer as described above requires the implementation of two functions with systolic arrays: a rank one update of the CSDM R_{mk} in terms of its Cholesky factor U_{mk} in Eq. (14) and the subsequent solution of a set of N linear equations of the form

$$U_{mk}^H \underline{h} = \underline{b} \tag{19}$$

as required by Eqs. (17) and (18).

Rank One Cholesky Factor Update [5,6]: Let the N-dimensional row vector

$$\underline{z} = (1 - \mu)^{1/2} \underline{x}_m^H \tag{20}$$

$$= [z_1 \; z_2 \; \ldots \; z_N] \tag{21}$$

and the upper triangular N-by-N matrix

$$U = \mu^{1/2} U_{m,k-1} \tag{22}$$

be defined. Now form the (N + 1)-by-N data augmented Cholesky matrix

$$B = \begin{bmatrix} - \underline{z} - \\ U \end{bmatrix} = \begin{bmatrix} z_1 & z_2 & \cdots & z_N \\ u_{11} & u_{12} & \cdots & u_{1N} \\ 0 & u_{22} & \cdots & u_{2N} \\ \vdots & \vdots & & \\ 0 & 0 & \cdots & u_{NN} \end{bmatrix}, \tag{23}$$

which can be reduced to upper triangular form by a sequence of N orthogonal plane rotations indicated by the orthogonal premultiplier matrix P as

$$PB = \begin{bmatrix} \bar{U} \\ - - - \\ \underline{0}^T \end{bmatrix} \tag{24a}$$

$$= \begin{bmatrix} \bar{u}_{11} & \bar{u}_{12} & \cdots & \bar{u}_{1N} \\ 0 & \bar{u}_{22} & \cdots & \bar{u}_{2N} \\ \vdots & \vdots & & \vdots \\ 0 & 0 & \cdots & \bar{u}_{NN} \\ 0 & 0 & & 0 \end{bmatrix} \tag{24b}$$

where $P = P_N P_{N-1} \cdots P_1$, $P_n^H P_n = I$ and $\underline{o}$ is an N-vector of all zeroes. Thus,

$$B^H P^H P B = B^H B \tag{25a}$$

$$= U^H U + z^H z \tag{25b}$$

$$= \mu U_{m,k-1}^H U_{m,k-1} + (1 - \mu)\underline{x}_m \underline{x}_m^H \tag{25c}$$

$$= R_{mk} \tag{25d}$$

$$= U_{mk}^H U_{mk} \tag{25e}$$

$$= \bar{U}^H \bar{U} \tag{25f}$$

and U is the rank one updated Cholesky factor of the estimated CSDM R_{mk}. If u_{ii}, $1 \leq i \leq N$ is real, then u_{ii}, $1 \leq i \leq N$ is also real when the boundary cell process definition of figure 1 is used.

The systolic array realization of the rank one Cholesky factor update requires both a boundary cell and an internal cell as illustrated in figure 1. The specific linear systolic array for reduction of Eq. (23) to upper triangular form is given in figure 2. It is the boundary cell that must compute the correct plane rotation angle complex cosine and sine values (c,s) and the internal cells which propagate that rotation down the n-th row of the matrix $P_{n-1} P_{n-2} \cdots P_1 U$.

Linear Equation Back Solve [7]: The solution of Eq. (19) is performed as a sequential backsubstitution of the elements of h as they are obtained

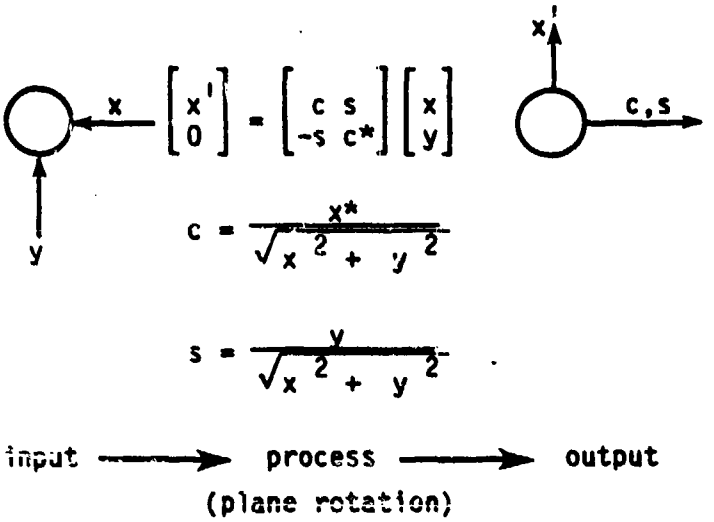

Figure 1A. Boundary Cell Input-Process-Output Diagram for Cholesky Factor Update (real y)

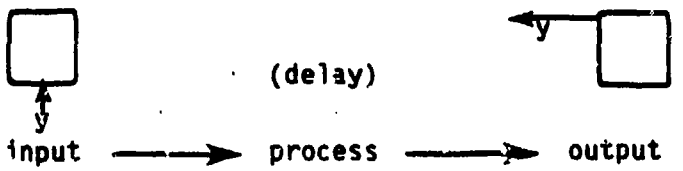

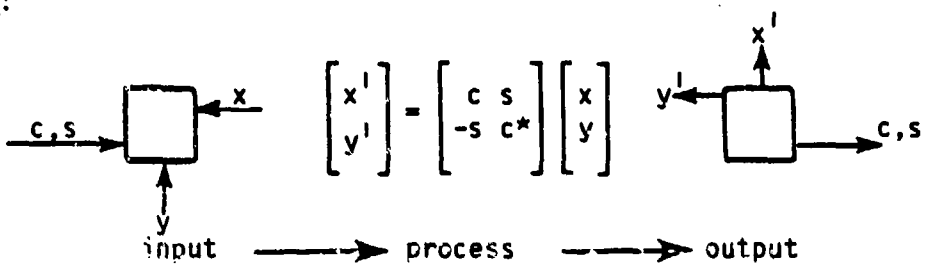

Figure 1B. Internal Cell Input-Process-Output Diagram for both the Delay and Compute Function Required for Cholesky Factor Update

Figure 1. Boundary Cell and Internal Cell Input-Process-Output Diagram for the Cholesky Factor Update

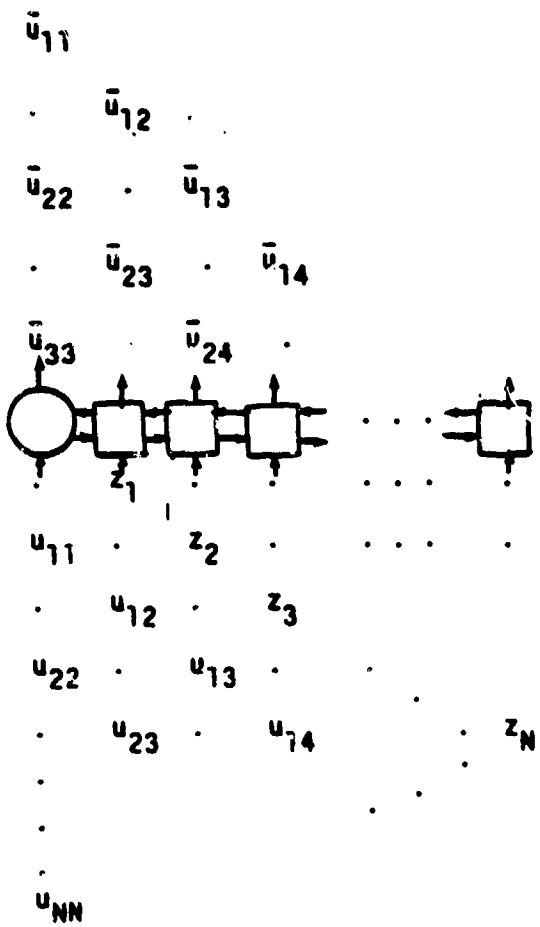

Figure 2. Linear Systolic Array for a Rank One Cholesky Factor Update

in sequence. Eq. (19) is of the form

$$\begin{bmatrix} u_{11} & 0 & 0 & \cdots & 0 \\ u_{12} & u_{22} & 0 & \cdots & 0 \\ u_{13} & u_{23} & u_{33} & \cdots & \cdot \\ \cdot & \cdot & \cdot & & \cdot \\ \cdot & \cdot & \cdot & & \cdot \\ u_{1N} & u_{2N} & u_{3N} & \cdots & u_{NN} \end{bmatrix} \begin{bmatrix} h_1 \\ h_2 \\ h_3 \\ \cdot \\ \cdot \\ h_N \end{bmatrix} = \begin{bmatrix} b_1 \\ b_2 \\ b_3 \\ \cdot \\ \cdot \\ b_N \end{bmatrix} . \tag{26}$$

Thus

$$\begin{aligned} h_1 &= b_1/u_{11} \\ h_2 &= (b_2 - u_{12}h_1)/u_{22} \\ h_3 &= (b_3 - u_{13}h_1 - u_{23}h_2)/u_{33} \\ &\vdots \\ h_N &= (b_n - u_{1N}h_1 - \cdots - u_{N-1,N}h_{N-1})/u_{NN} \end{aligned} \tag{27}$$

which is realized with an implementation of the linear systolic array using the cells illustrated in figure 3. The corresponding systolic array is shown in figure 4.

It is noted that systolic arrays for the rank one Cholesky update (figure 2) and linear equation backsolve solution (figure 4) are linear arrays with minor differences in input-output structure. As discussed above, utilization of the boundary and internal cells is fifty percent. One hundred percent utilization is achieved with the interleaving of two problems delayed by one cycle. Moreover, it is possible using a nonalgebraic, i.e., geometric approach, to partition large (N) problems into segments wherein a smaller systolic array of size less than N internal cells can be time multiplexed.

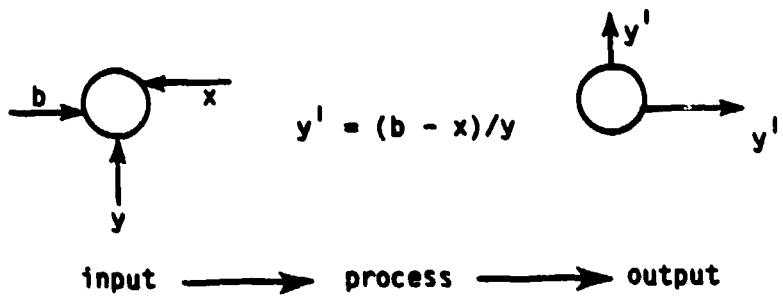

Figure 3A. Boundary Cell Input-Process-Output Diagram
for Linear Equation Backsubstitution

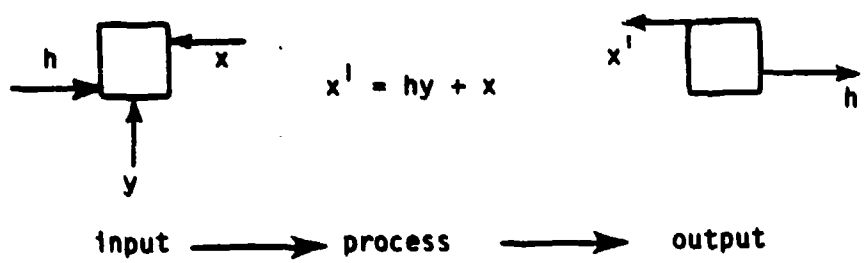

Figure 3B. Internal Cell Input-Process-Output Diagram
for Linear Equation Backsubstitution

Figure 3. Linear Equation Backsubstitution

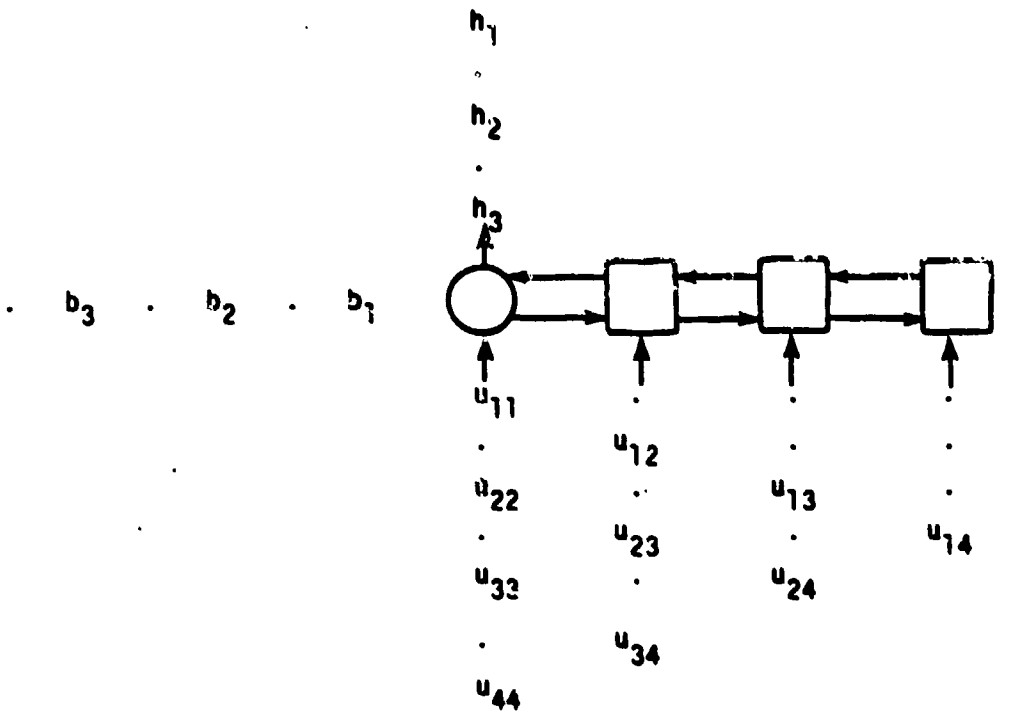

Figure 4. Systolic Array for Solution of Linear Equations by Backsubstitution for a 4-Element Partition

PERFORMANCE OF AN MVDR BEAMFORMER

The CSDM for an array that receives both a signal with autopower spectral density (ASD)σ_s^2 and an interference, which is uncorrelated with the signal, and an ASD σ_i^2 at frequency f is given by

$$R = \sigma_s^2 \underline{d}_s \underline{d}_s^H + \sigma_i^2 \underline{d}_i \underline{d}_i^H + \sigma_o^2 I. \tag{28}$$

In Eq. (28), σ_o^2 is the spatially uncorrelated noise ASD at frequency ω, I is an N-by-N identity matrix, and $\underline{d}_s$ and $\underline{d}_i$ are the steering vectors for the signal and interference, respectively. The interference is assumed to be in the farfield of the array, i.e., it is a Point INterference (PIN) with respect to angle of arrival.

The MVDR filter vector for beamforming in the signal direction at frequency ω has been shown to be

$$\underline{w} = R^{-1} \underline{d}_s / \underline{d}_s^H R^{-1} \underline{d}_s \ . \tag{29}$$

For a conventional time delay-and-sum beamformer (CBF) the vector $\underline{d}_s$ is used. The gain in signal to the total of interference and noise power at the beam output relative to a single sensor is given by

$$G_{MV} = (\sigma_s^2 |\underline{w}^H \underline{d}_s|^2 / \underline{w}^H [\sigma_i^2 \underline{d}_i \underline{d}_i^H + \sigma_o^2 I] \underline{w}) / (\sigma_s^2 / [\sigma_i^2 + \sigma_o^2]) \tag{30}$$

for the MVDR beamformer and

$$G_C = (\sigma_s^2 N^2 / \underline{d}_s^H [\sigma_i^2 \underline{d}_i \underline{d}_i^H + \sigma_o^2 I] \underline{d}_s) / (\sigma_s^2 / [\sigma_i^2 + \sigma_o^2]) \tag{31}$$

for the CBF. The array gain improvement (AGI) of the MVDR relative to the CBF is

$$AGI = G_{MV}/G_c$$

$$= 1 + \frac{r^2 \ell(1-\ell)}{1+r} \tag{32}$$

where

$$r = N\sigma_i^2/\sigma_o^2 \tag{33}$$

and represents the interference to uncorrelated noise variance ratio at the output of a CBF steered with its main response axis (MRA) directly at the interference. The parameter ℓ ($0 \leq \ell \leq 1$) is defined by the expression

$$\ell = |\underline{d}_s^H \underline{d}_i|^2/N^2. \tag{34}$$

Figure 5 gives the AGI as a function of r for four different values of ℓ; namely, $\ell = 1/2$ (-3 dB), $\ell = 2/100$ (-17 dB), $\ell = 5/1000$ (-23 dB) and $\ell = 1/1000$ (-30 dB). For either high interference levels and/or low noise levels, significant gains of greater than 10 dB are achievable with MVDR beamforming over a CBF. At high noise levels the increased uncorrelated noise begins to mask the PIN as the major degrading factor and useful AGII is only achieved when the PIN is inside the mainlobe of the beam receiving the signal (-3 dB re MRA).

ADAPTIVE BEAMFORMING FOR VERY LARGE ARRAYS

The fundamental parameter which determines the signal to total background noise variance ratio gain for an array is the number of sensors

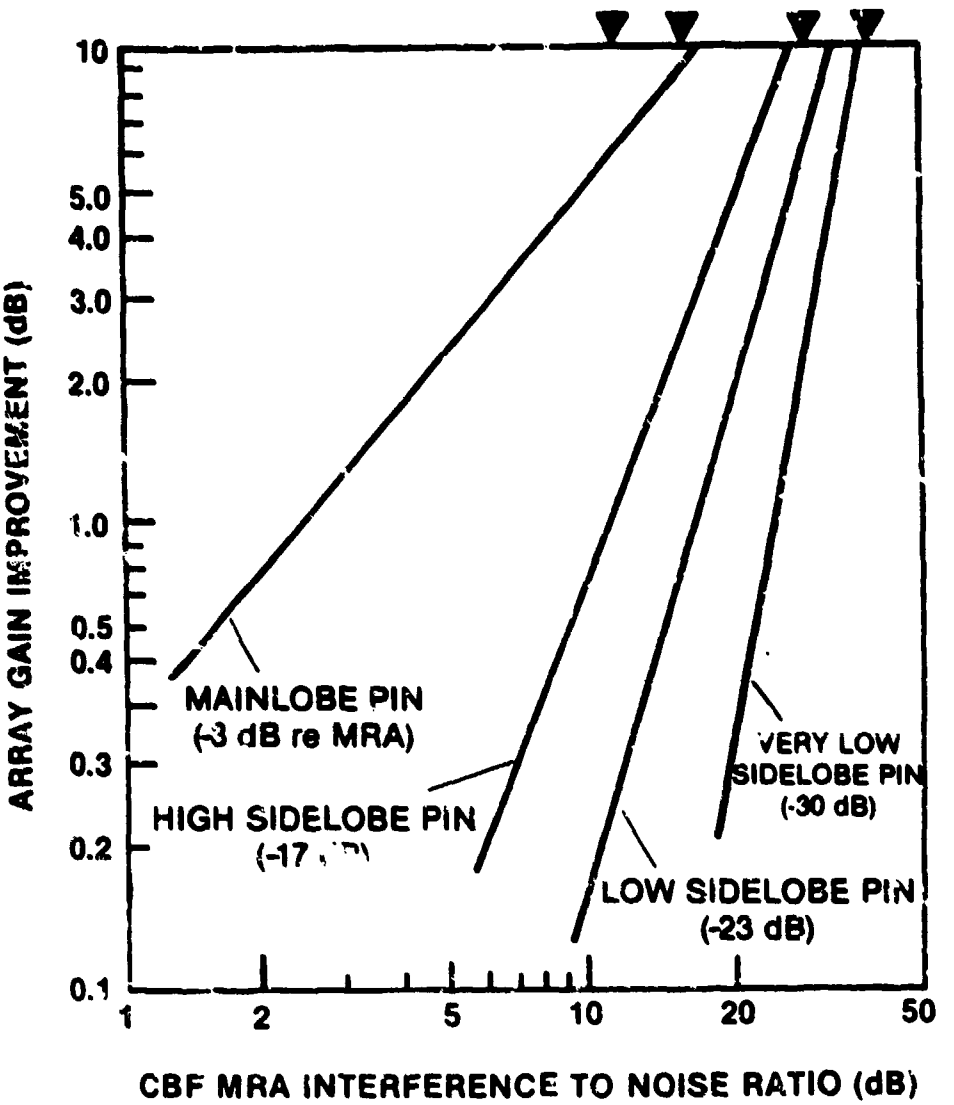

Figure 5. Minimum Variance Optimum Beamformer AGI Relative to a CBF as a Function of the Interference-to-Noise Ratio for a PIN Measured at the Output of a CBF Steered Directly at the Interference

N. Simply stated, if an array cannot provide a certain level of required conventional beamformer array gain with only spatially uncorrelated white noise present, then adaptive beamforming will not alter this fact and the only option is to make the number of sensors (N) in the array larger. To illustrate this point it is observed that

$$G_{MV}|_{\sigma_i^2 = 0} = G_c|_{\sigma_i^2 = 0} \tag{35}$$

$$= N .$$

Thus, from the array gain perspective, CBF is optimum when there is no interference present and the only recourse is to build larger arrays, i.e., arrays with more sensors.

Given the specific spatially uncorrelated white noise array gain, N, of Eq. (35) for an array of N sensor elements, an implementation of the MVDR beamformer described previously requires the update of an N dimensional Cholesky factor and the solution of a correspondingly large set of linear equations. Thus, the number of sensor elements N equal to the array white noise gain determines the size of the element space MVDR system. For arrays with a large number of sensor elements N, the computational requirements can become prohibitive given that the computing burden is proportional N^3 as specified by Eq. (12).

In a dynamic situation, where the angle of arrival for a particular interference is changing with time, the effective averaging time for estimating the interelement CSDM Cholesky factor is limited by a temporal stationarity assumption. Thus, the variance of the elements in the CSDM estimator of Eq. (11), which is inversely proportional to averaging time, has a lower bound determined by the finite averaging time. Specifically, if M is the effective number of statistically independent sample vectors, $\underline{x}_m$, which are exponentially averaged to produce the estimated CSDM of Eq. (11), then the variance on the MVDR beam output power estimator detection statistic of Eq. (10) is inversely proportional to M - N + 1 where it is

assumed that M > N [Refs. 8, 9]. Thus, as the number of elements (N) in the array increases, it is necessary to increase the CSDM estimator averaging time as determined by M proportionately to maintain the same beam output power estimator variance.

Eventually, for the element space MVDR process, the size of the array N is limited by the time stationarity constraint which is, in turn, determined by the interference position rate of change with respect to time.

A natural way to avoid the temporal stationarity limitation on the white noise array gain N discussed above is to perform the systolic MVDR process in a domain other than the N-dimensional element space. If this new domain has a lower dimensionality, both the systolic engine computational and memory size complexity and the effective time averaging requirement constraints are reduced accordingly. References [10] and [11] suggest the implementation of the MVDR algorithm in a so-called beam space. In beam space, only spatially orthogonal CBF beams that are steered contiguous to a selected reference beam are used as inputs to an MVDR beam interpolation algorithm. Clearly, the question of selecting the appropriate number of and location for orthogonal beams is not straightforward. At a minimum, this selection is a frequency dependent process due to the variation of beam overlap caused by the increase of beamwidth with a decrease in frequency. In addition, the number of independent beams must be made large enough to provide a sufficient number of degrees of freedom for near optimum performance in a multiple interference condition.

As a practical matter, even the formation of a conventional time delay-and-sum beam for a very large array is a difficult implementation issue. Usually partial aperture, i.e., subarray, beams are formed as a first step in the formation of a full beam from a large array. An alternative to the beam space approach for dimensionality reduction in very large arrays is referred to herein as the subarray (SA) space formulation [Refs. 12, 13]. In this approach, subapertures of contiguous elements in the large array are prebeamformed using simple time delay-and-sum and fixed spatial windowing techniques. This partitioned subarray beamforming (SBF) can be envisioned as creating a secondary array of spatially directional

elements which, in turn, are processed with an N/P-dimension MVDR beamformer in cascade with the subaperture beamformers discussed above.

If each of the partitioned subarrays (N/P), as illustrated in figure 6, consists of P contiguous sensor elements, then the MVDR process is of dimension N/P. However, as with the beam space approach, more than one small (dimension N/P) CSDM Cholesky factor needs to be estimated at each frequency. This is in contrast with the element space MVDR where a single very large (dimension N) CSDM Cholesky factor is estimated. This is because each SBF can form approximately P spatially independent beams which resolve substantially nonoverlapping segments of solid angle. Thus, for the formation of a particular CSDM matrix estimator, those SBF outputs steered at the same angle should be selected. This SA space requirement would constitute a need for approximately P MVDR parallel processes each of dimension N/P as opposed to one MVDR process of dimension N required for the element space formulation. It is noted that from the computational requirement standpoint the SA space burden is proportional to $B_{SA} = (N/P)^2 N$ as contrasted to $B_E = N^3$ for element space. The actual burden is proportional to $[(N/P)^2 P + (N/P)^2 N] \quad (N/P)^2 N$ for $N >> P$. The Cholesky factor update burden is $(N/P)^2 P$ and the backsubstitution burden is $(N/P)^2 N$. Thus, the computational load and memory size reductions can be enormous when the SA space is adopted. Moreover, the restriction on the effective averaging time M imposed by the array size N becomes $M - (N/P) + 1 \geq T$, where T is a threshold set by the desired variance of the beam output power detection statistic. It follows that averaging time can be reduced in a SA space formulation to accommodate the spatial dynamics of the interference with essentially no loss of performance.

The beam and SA space MVDR array gain performance is obtained by

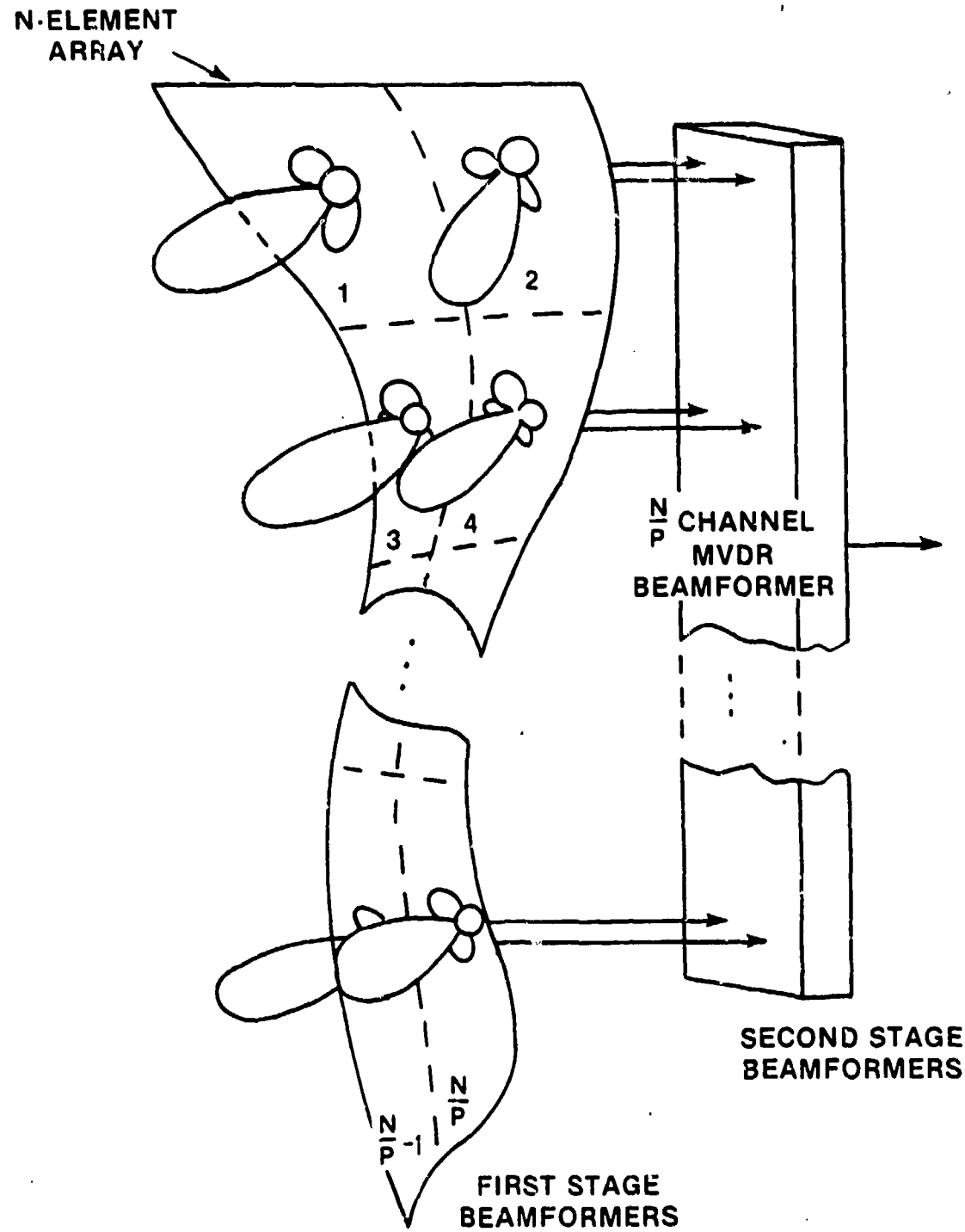

Figure 6. Subarray Space Partitioning and Cascaded Beamforming of a Very Large N-Element Array to Reduce N/P-Input MVDR Beamformer Complexity and Convergence Time Restrictions. (Each of the (N/P) subarrays consists of P elements with conventional beamforming.)

introducing the array element data preprocessing matrix

$$D = \begin{cases} \left[\underline{d}_{-L/2} \quad \cdots \quad \underline{d}_0 \quad \cdots \quad \underline{d}_{L/2}\right] & \text{for beamspace} \qquad (36a) \\ \begin{bmatrix} \underline{d}_{s1} & \underline{0} & \cdots & \underline{0} \\ \underline{0} & \underline{d}_{s2} & & \underline{0} \\ \vdots & \vdots & \ddots & \\ \underline{0} & \underline{0} & & \underline{d}_{s,N/P} \end{bmatrix} & \text{for SA space.} \qquad (36b) \end{cases}$$

In Eq. (36a), $\underline{d}_k$ is a CBF N-dimensional steering vector corresponding to a beam space patch of size L+1 which is defined as being centered at a point, Θ, specified by a reference beam which has steering vector $\underline{d}_0 = \underline{d}_0(\Theta)$. Ideally, these steering vectors are assumed to be orthogonal, i.e., $\underline{d}_i^H \underline{d}_j = N\delta_{ij}$. For the SA space MVDR process, the P-dimensional vector $\underline{d}_{sk}$ corresponds to the P-element subvector of the N-dimensional steering vector

$$\underline{d}_0 = \begin{bmatrix} \underline{d}_{s1} \\ \underline{d}_{s2} \\ \vdots \\ \underline{d}_{s,N/P} \end{bmatrix}, \qquad (37)$$

which would be required to electronically steer the entire array subarray by subarray at a single point that is implicit in the steering vector $\underline{d}_0$. For the beam space formulation D is an N-by-(L+1) dimensional matrix and for the subarray counterpart D is of dimension N-by-(N/P). If (L+1) = N/P for these two suboptimum MVDR processes and the same AGI performance results, then the two approaches would require the same hardware implementation with identical performance except that the beamspace process requires full

conventional beams to be formed instead of only partial beams.

To establish the MVDR AGI for the two suboptimum procedures, the reduced dimension CSDM matrix

$$\bar{R} = D^H K D \tag{38}$$

is defined. For both the beam space and SA space processes, the secondary beam output variance

$$\sigma_b^2 = \underline{\bar{w}}^H \bar{R} \underline{\bar{w}} \tag{39}$$

is minimized with respect to either the (L+1) or (N/P) dimensional vector $\underline{w}$. The constraints that the element in location (L/2)+1 of $\underline{w}$ be unity for the beamspace and

$$N = \underline{\bar{w}}^H \underline{D}^H \underline{d} \tag{40}$$

for the SA space procedures are required to satisfy the distortionless signal constraint.

It is a direct procedure to obtain the following AGI expressions

$$AGI_b = 1 + \frac{r^2 \ell([L+1]\bar{\ell}-\ell)}{1 + r[L+1]\bar{\ell}}, \tag{41a}$$

and

$$AGI_s = 1 + \frac{r^2 \ell(\ell_s-\ell)}{1 + r\ell_s} \tag{41b}$$

for the beam space and SA counterparts, respectively, to Eq. (32) which corresponds to the fully optimum element space configuration. In Eq. (41a),

$$[L+1]\bar{\ell} = \sum_{k=-\frac{L}{2}}^{\frac{L}{2}} \ell_k \tag{42}$$

where $\ell_k = |\underline{d}_i^H \underline{d}_k|^2 / N^2 (0 \leq \ell_k \leq 1)$ is the relative response level of the interference in the k-th beam output of the beam space patch. The quantity $\bar{\ell}$ can be thought of as the interference response level averaged over all (L+1) beams in the beam space patch. In Eq. (41b), ℓ_s $(0 \leq \ell_s \leq 1)$ is the relative response level of the interference in the SA beam output. Note that in the limiting case for SA MVDR processing, P=1 corresponds to only one sensor per SA. Here the SA has an omnidirectional response so that ℓ_s = 1 and the result is the same as Eq. (32) as expected. It is observed that for the two suboptimum MVDR processes to perform equally, then

$$\begin{aligned} e &= \ell_s \\ &= [L+1]\bar{\ell} \end{aligned} \tag{43}$$

and optimality is approached only to the extent that e approaches unity. Figure 7 gives the AGI metric

$$AGI(e) = 1 + \frac{r^2 \ell (e - \ell)}{1 + re}$$

for the suboptimum, reduced dimension beam and subarray space MVDR processes for several values of e. The same values of the interference response

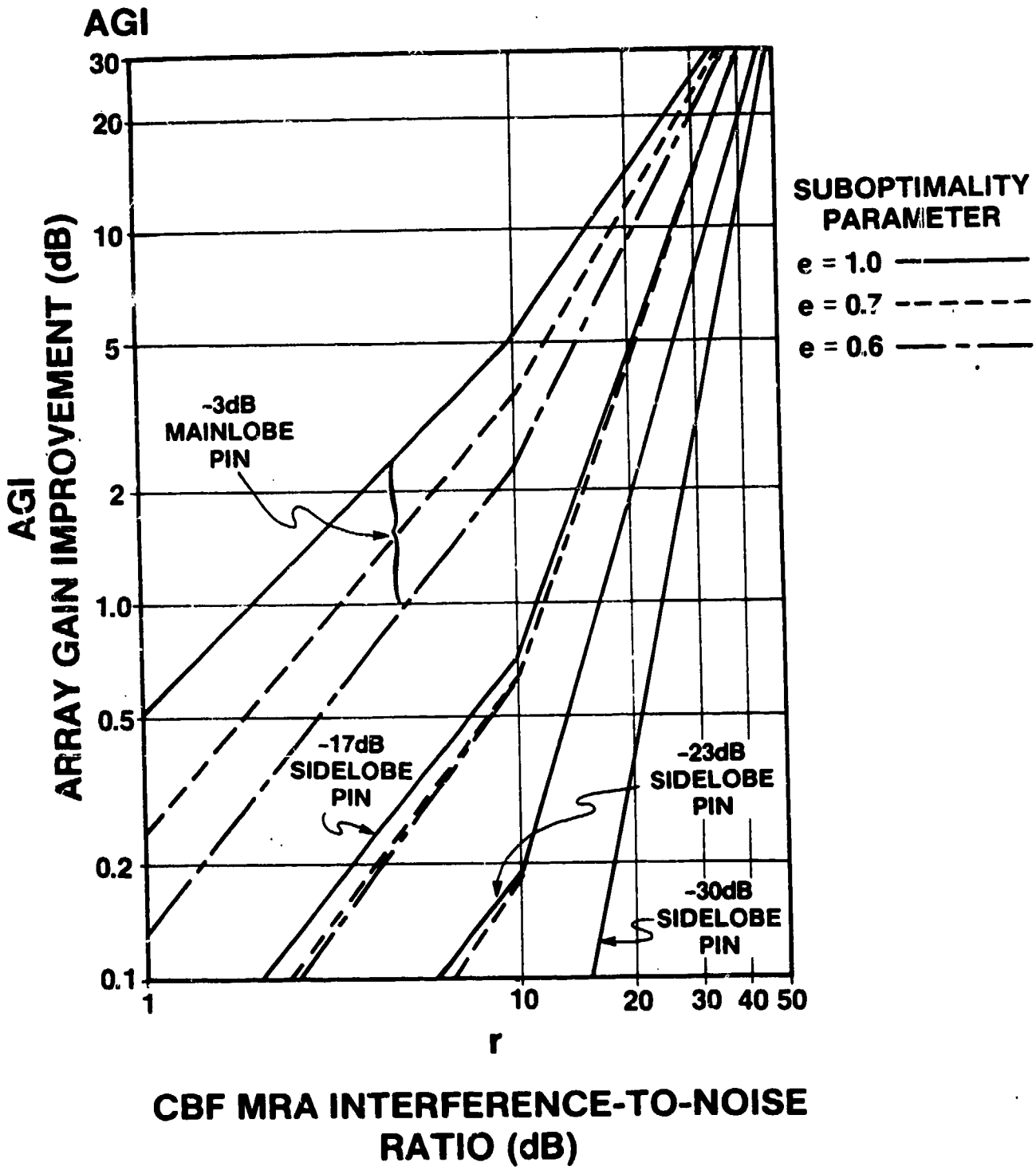

Figure 7. Comparison of Suboptimum (Subarray and Beam Space) and Optimum (Element Space) MVDR Process AGI Versus Interference-to-Noise Ratio.

level, ℓ, for the full aperture CBF are used as in Figure 5. It is significant that at high interference-to-noise levels (r) the suboptimum procedures are nearly equivalent to the optimum element based process except for $\ell = 1/2$. Furthermore, it is primarily only for large r that substantial sidelobe interference AGI is obtained. For mainlobe PIN, when $\ell = 1/2$ the beamspace MVDR would have a substantial performance loss. This is because e only differs from 1/2 by the average sidelobe level of the interference over the remaining beams in the patch and this would be a small number. Thus, for interference within the mainlobe subarray MVDR would be superior.

CONCLUSIONS

The fundamentals of adaptive beamformer (ABF) implementation using systolic computing arrays has been presented. It has been shown that for a continuously updating ABF, a direct open loop realization can be obtained with a linear systolic array consisting of just two types of functional computing cells. The performance of a generic ABF system has been reviewed. Finally, the problem of computational burden, memory requirements, and extreme convergence time associated with arrays having large numbers of elements has been addressed by showing that systolic array techniques need be applied only at the second stage of a cascaded beamformer. The tremendous saving in MVDR implementation hardware with application of the suboptimum processes could offset the loss of performance. The preferred suboptimum MVDR processes use subarray prebeamforming because it is extremely regular in its architecture; it is not frequency-dependent; and it yields better AGI performance for the same MVDR complexity.

REFERENCES

1. S. Haykin, J. Justice, N. Owsley, and A. Kak, Array Signal Processing, Prentice-Hall, 1985.

2. T. Kailath, S. Y. Kung, and H. Whitehouse, VLSI and Modern Signal Processing, Prentice-Hall, 1985.

3. H. T. Kung, "Why Systolic Arrays," IEEE Trans. Computers, 15 (1), pp. 37-46, 1982.

4. Y. S. Kung et al., "Wavefront Array Processor: Language, Architecture, and Applications," IEEE Trans. Computers, C-31, pp. 1054-1066, 1982.

5. P. Kuekes, J. Avila, and D. Kandle, Adaptive Beamforming Design Specification, ESL Inc., Sunnyvale, CA, 20 May 1986.

6. R. Schreiber and Wei-Pai Tang, "On Systolic Arrays for Updating the Cholesky Factorization," Royal Institute of Technology, Stockholm, Sweden, Dept. of Numerical Analysis and Comp. Science, TRITA-NA-8313, 1984.

7. G. Strang, Linear Algebra and It's Applications, Academic Press, 1980, Second Edition.

8. J. Capon and N. Goodman, "Probability Distributions for Estimators of Frequency Wavenumber Spectrum," Proc. IEEE, Vol. 58, pp. 1785-1786, 1970.

9. J. Capon, "Correction to Ref. [8]," Proc. IEEE, Vol. 59, p. 112, 1971.

REFERENCES (Cont'd)

10. A. H. Vural, "A Comparative Performance Study of Adaptive Array Processors," Proceedings of IEEE ICASSP, Hartford, CT, 1977, pp. 695-700.

11. D. A. Gray, "Formulation of the Maximum Signal-to-Noise Ratio Array Processor in Beam Space," J. Acoust. Soc. Am., 72 (4), October 1982, pp. 1195-1201.

12. N. L. Owsley and Law, J. F., "Dominant Mode Power Spectrum Estimation," Proceedings of IEEE ICASSP, Paris, April, 1982, Vol. 1, pp. 775-779.

13. N. L. Owsley, "Signal Subspace Based Minimum-Variance Spatial Array Processing," Proceedings of Asilomar Conf. on Circuits, Systems, and Computers, November 6-8, 1985, pp. 94-97.

INITIAL DISTRIBUTION LIST

Addressee	No. of Copies
NAVSEASYSCOM (PMS 402; 63D, CDR L. Schneider, Dr. C. Walker, Mr. D. Early, Dr. Y. Yam; PMS 409; PMS 412, P. Mansfield; PMS 418, CAPT E. Graham III)	8
NORDA (R. Wagstaff, B. Adams)	2
CNR (OCNR-10, -11, -12, -122, -127, -20)	6
ONT (OCNR-231, Dr. T. Warfield, Dr. N. Booth, Dr. A. J. Faulstich, CAPT R. Fitch)	5
DARPA (Dr. R. H. Clark, Dr. C. Stuart, Dr. A. Ellinthrope)	3
SPAWAR (PDW-124; PMW-180T, Dr. J. Sinsky)	2
NOSC (G. Monkern)	1
NASC (NAIR-340)	1
SUBBASE, GROTON (FA10)	1
DTIC	12
APL/Johns Hopkins	1
APL/U. Washington	1
ARL/Penn State	1
ARL/U. Texas	1
MPL Scripps	1
Woods Hole Oceanographic Institution	1
ESL/TRW, Inc. (B. Chaterjee) Contract No. N0000140-83-C-0110	4